THE JOURNAL OF BIOLOGICAL CHEMISTRY VOL. 286, NO. 32, pp. 28533–28543, August 12, 2011

Retinoic Acid Signaling Sequentially Controls Visceral and Heart Laterality in Zebrafish*[S]

Received for publication, March 27, 2011, and in revised form, June 1, 2011 Published, JBC Papers in Press, June 13, 2011, DOI 10.1074/jbc.M111.244327

Sizhou Huang[‡§], Jun Ma[‡§], Xiaolin Liu[‡§], Yaoguang Zhang[‡], and Lingfei Luo[‡§1]

From the [‡]Key Laboratory of Freshwater Fish Reproduction and Development, Ministry of Education, and the [§]Laboratory of Molecular Developmental Biology, School of Life Sciences, Southwest University, Beibei, 400715 Chongqing, China

During zebrafish development, the left-right (LR) asymmetric signals are first established around the Kupffer vesicle (KV), a ciliated organ generating directional fluid flow. Then, LR asymmetry is conveyed and stabilized in the lateral plate mesoderm. Although numerous molecules and signaling pathways are involved in controlling LR asymmetry, mechanistic difference and concordance between different organs during LR patterning are poorly understood. Here we show that RA signaling regulates laterality decisions at two stages in zebrafish. Before the 2-somite stage (2So), inhibition of RA signaling leads to randomized visceral laterality through bilateral expression of *nodal*/*spaw* in the lateral plate mesoderm, which is mediated by increases in cilia length and defective directional fluid flow in KV. Fgf8 is required for the regulation of cilia length by RA signaling. Blockage of RA signaling before 2So also leads to mild defects of heart laterality, which become much more severe through perturbation of cardiac *bmp4* asymmetry when RA signaling is blocked after 2So. At this stage, visceral laterality and the left-sided Nodal remain unaffected. These findings suggest that RA signaling controls visceral laterality through the left-sided Nodal signal before 2So, and regulates heart laterality through cardiac *bmp4* mainly after 2So, first identifying sequential control and concordance of visceral and heart laterality.

During vertebrate development, left-right (LR)[2] asymmetry is evident both in heart and visceral organs such as liver, pancreas, and gut. *Situs inversus totalis*, in which there is complete right to left reversal of the thoracic and abdominal organs, occurs once in about 8,000 persons. Although *situs inversus* is usually of no medical consequence, heterotaxia, incomplete reversal of organs, occurs with higher frequency and causes significant medical problems. These problems are observed not only in humans but also in nearly all vertebrates in whom LR asymmetry needs to be established during development. In zebrafish, LR asymmetric signals are first established around KV, a ciliated organ that generates directional fluid flow (1–3). Ciliogenesis, key to the initiation of LR asymmetry, is dependent on fibroblast growth factor (FGF) signaling (4, 5). Then, LR asymmetry is conveyed and stabilized in the lateral plate mesoderm (LPM), patterning left and right sides of the embryo (6). A critical event of LR patterning at this stage is the left-sided expression of *nodal*/*southpaw* (*spaw*) in the LPM (7–11). The left-sided Nodal/Spaw then activates *lefty1* in the ventral neural tube, *lefty2* and *pitx2* in the LPM, all exclusively on the left side (12–15). Lefty1 and Lefty2 antagonize Nodal activity, thus generating a negative feedback loop to restrict the extent and duration of Nodal signaling. The left-sided expression of *nodal/spaw, lefty2*, and *pitx2* are highly conserved in vertebrates to ensure proper LR patterning (6).

Retinoic acid (RA) and bone morphogenetic protein signals have been reported to regulate several aspects of LR asymmetry. Treatment of RA antagonist leads to randomization of heart looping and perturbed sideness of *nodal* in mouse (16), but roles of RA signaling in the determination of heart and visceral laterality in zebrafish remain unknown. In *Xenopus*, chick, and mouse, bone morphogenetic protein signaling is required to repress Nodal activity in the right LPM, thus ensuring right-sided laterality (17–20). In zebrafish, bone morphogenetic protein signaling regulates LR asymmetry at two distinct developmental time points. Shortly after KV has been formed during early segmentation, bone morphogenetic protein signaling is necessary to repress *spaw* in the right LPM, similar to other vertebrates (21). In later segmentation at around the 22-somite (22So) stage prior to the initiation of cardiac jogging, *bmp4* is asymmetrically distributed in the cardiac field with stronger expression on the left side (22). This asymmetric *bmp4* is required for the determination of heart laterality (21–23).

Ectopic expression of *bmp4* on the right side results in reversal of heart laterality, but visceral organs are unaffected (24). Induction of exogenous *noggin3* at the 16-somite stage causes perturbation of heart laterality, but visceral laterality remains normal (21). High occurrence of heterotaxia in nature proposes that asymmetries of heart and visceral organs may involve different regulatory mechanisms and need to be coordinated. However, key mechanistic differences and concordance between visceral and heart laterality during LR patterning remain to be elucidated.

Here we demonstrate that inhibition of RA signaling before 2So leads to randomized laterality of visceral organs through bilateral expression of *spaw*, which resulted from increases in

* This work was supported by National Basic Research Program of China Grant 2009CB941200, National Natural Science Foundation of China Grant 30925022, Program for Changjiang Scholars and Innovative Research Team Program Grant IRT0859, Program for New Century Excellent Talents (NCET) Program Grant NCET-07-0713, CQ Chongqing Science and Technology Commission Grant 2009BA5041, Southwest University Grant Kb2009008, and the Par-Eu Scholars Program.

[S] The on-line version of this article (available at http://www.jbc.org) contains supplemental Movies S1 and S2, Figs. S1–S7, and Tables S1–S5.

[1] To whom correspondence should be addressed. Tel.: 86-23-68367957; Fax: 86-23-68367958; E-mail: lluo@swu.edu.cn.

[2] The abbreviations used are: LR, left-right; LPM, lateral plate mesoderm; DEAB, 4-diethylaminobenzaldehyde; MO, morpholino oligo; RA, retinoic acid; So, somite stage; DMSO, dimethyl sulfoxide; hpf, hours post-fertilization; E, epiboly stage.

cilia length and defective directional fluid flow in KV. Fgf8 is required to mediate the control of cilia length by RA signaling. Inhibition of RA signaling before 2So also results in mild defects of heart laterality, which become much more severe through disturbance of cardiac *bmp4* asymmetry when RA signaling is blocked after 2So. However, visceral laterality and left-sided *spaw* and *lefty2* remain unaffected at this stage. Our study first identifies RA signaling as the key signaling pathway that sequentially controls visceral and heart laterality, so that RA signaling achieves their concordance during LR patterning.

EXPERIMENTAL PROCEDURES

Zebrafish Strain—Zebrafish (*Danio rerio*) of the AB genetic background, *gutGFP*, *2CLIP*, and *Tg*(*cmlc2*:*GFP*) lines were raised and maintained under standard laboratory conditions.

BMS453, 4-Diethylaminobenzaldehyde (DEAB), and RA Treatment—Zebrfish embryos were incubated with 0.4 μM BMS453 (0.8 μl of 10 mM BMS453 stock diluted in 20 ml of egg water, Bristol-Myers Squibb), 1 μM DEAB (2 μl of 10 mM DEAB stock diluted in 20 ml of egg water, Sigma), or 0.05 μM RA (0.8 μl of 1.25 mM RA stock diluted in 20 ml of egg water, Sigma) in different time frames. 1 nM RA was applied to rescue DEAB. Treated embryos were washed twice and cultured in egg water until fixation or observation. In all experiments, treated embryos were compared with mock treated control siblings (0.8 μl of DMSO diluted in 20 ml of egg water).

Morpholinos and mRNAs—Fluorescein-labeled antisense morpholinos (Gene Tools) against *bmp4* (*bmp4MO*, 5′-GGTGTTTGATTGTCTGACCTTCATG-3′; 200 μM) (21) or *spaw* (*spawMO*, 5′-GCACGCTATGACTGGCTGCATTGCG-3′; 1 mM) (11), *fgf8* (*fgf8MO*, 5′-TGAGTCTCATGTTTATAGCCTCAGT-3′; 100 or 60 μM) (25) were applied. *bmp4MO* was injected into the cell body of one cell of *Tg*(*cmlc2*:*GFP*) transgenic embryos at the 8–32-cell stage. Embryos with different distributions of the morpholino were checked at the 64-cell as well as the shield stages, and sorted at 10So according to fluorescein epifluorescence. *GFP* and *spaw* mRNAs were synthesized from linearized plasmid templates using the Message Machine Kit (Ambion), and co-injected into the cell body of one cell of *2CLIP* transgenic embryos at the 4–16-cell stage. Embryos with different distributions of mRNAs were sorted at the shield stage and confirmed at 10So according to GFP epifluorescence.

Quantitative Real Time PCR—First strand cDNA synthesis was performed using OmniScript RT kit (Qiagen). Then, quantitative PCRs were performed for *fgf8* (5′-GAGGCTATAAACATGAGACTCATAC-3′, 5′-CGAACTCGACTCCCAAATGTGTC-3′); *erm* (5′-GTGAGAAGCAAGCGACATGGATG-3′, 5′-GAGTCTCTGCTCTTGTCCACATG-3′); and *pea3* (5′-CATGGATTATAAGATGGATGGATATC-3′, 5′-GTTCTCTGAGTGAAAGTCAGGAAC-3′) using the QuantiFast SYBR Green PCR kit (Qiagen) and a Realplex^2 Mastercycler (Eppendorf). Transcription of *β-actin* (5′-CATGGATGAGGAAATCGCTGCC-3′, 5′-GCTCAGGATACCTCTCTTGCTC-3′) was used for normalization.

Whole Mount in Situ Hybridization, Section, and Immunostaining—One-color whole mount *in situ* hybridization was performed as previously described (26), using established antisense probes (4, 21, 22, 27, 28).

For sectioning, *in situ* hybridized embryos were re-fixed in 4% paraformaldehyde in PBS, followed by incubation in 15 and 30% sucrose in 0.1% Tween/phosphate buffered saline for 2 h each. Then, embryos were mounted in 1.5% agarose in 30% sucrose, and balanced in 30% sucrose solution overnight at 4 °C. The mounted embryo was re-mounted in OCT (Sakura), sectioned using a CM1850 cryostat (Leica), and counterstained with DAPI. Images were captured at room temperature using AxioVision4 software (Carl Zeiss, Inc.), and a ×20/0.8 N.A. Plan Apochromat air objective mounted on an AxioImageZ1 microscope (Carl Zeiss, Inc.) equipped with MRc5 and MRm digital cameras (Carl Zeiss, Inc.). Whole mount immunostaining was performed to detect cilia in KV with anti-acetylated tubulin antibodies (Sigma) (4) and counterstained with DAPI as previously described.

Fluid Flow Observation—Fluorescent yellow-green latex beads (Sigma) were diluted 1:10 and injected into the KV of embryos at the 6–8-somite stage, which were subsequently mounted in 1.2% low melting point agarose (Invitrogen) in egg water. Images were captured at room temperature using LAS AF software (Leica), and a ×20/0.70 N.A. HC Plan Apochromat air objective mounted on a Leica SP5 confocal microscope (Leica).

Microscopy—In situ hybridized, immunostained, *gutGFP*, and *2CLIP* embryos were mounted in glycerol, whereas living *Tg*(*cmlc2*:*GFP*) transgenic embryos were mounted in 1.2% low melting point agarose (Invitrogen) in egg water. Images were captured at room temperature using AxioVision4 software (Carl Zeiss, Inc.), and a ×10/0.45 N.A. Plan Apochromat air objective mounted on an AxioImageZ1 microscope (Carl Zeiss, Inc.) equipped with MRc5 and MRm digital camera (Carl Zeiss, Inc.). Confocal images were captured at room temperature using LAS AF software (Leica), a ×20/0.70 N.A. HC Plan Apochromat air objective (Leica) and a ×40/1.2 N.A. C-Apochromat water objective (Carl Zeiss, Inc.) mounted on a Leica SP5 confocal microscope (Leica).

RESULTS

Stage-dependent Effects of RA Antagonist on Visceral and Heart Laterality—In zebrafish, treatments of exogenous RA or RA antagonist cause strong defects in exocrine pancreas differentiation and expansion (29). When we incubated *gutGFP* transgenic zebrafish embryos with the pan-retinoic acid receptor antagonist BMS-189453 (BMS453) (30, 31), we found that inhibition of RA signaling not only affected exocrine pancreas differentiation, but also led to LR defects of visceral organs. However, phenotypes of visceral laterality were dependent on the stage of BMS453 treatment (Fig. 1, *A–D*). To further investigate the regulatory stage of RA signaling on visceral laterality, effects of BMS453 treatment on the LR patterning of visceral organs were analyzed using the *2CLIP* transgenic line with liver and pancreas clearly labeled (32). Titrations of BMS453 at various times identified that BMS453 treatment from the 32-cell stage (32-cell) to 2So resulted in maximal reversal of visceral

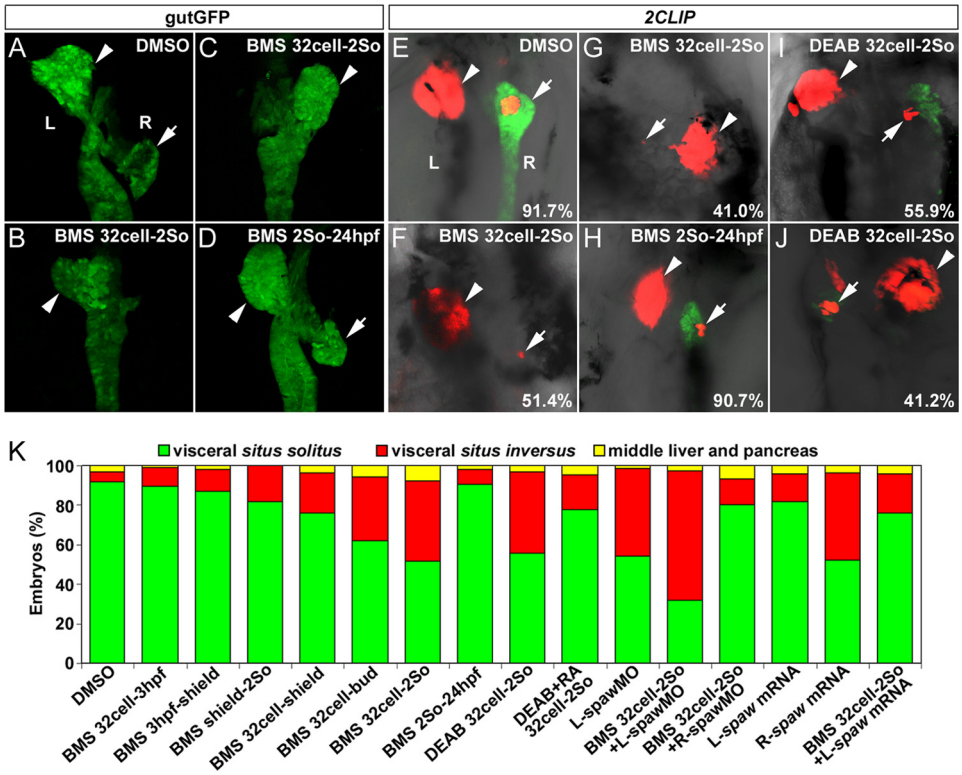

FIGURE 1. **Stage-dependent effects of RA antagonists on visceral laterality.** *A–D,* in contrast to control embryos treated with DMSO (*A*), embryos treated with BMS453 from 32-cell to 2So not only exhibited defective differentiation and morphogenesis of visceral organs, but also showed aberrant visceral laterality (*B* and *C*). Embryos treated with BMS453 from 2So to 24 hpf exhibited normal visceral laterality (*D*). The *gutGFP* line was used and observed at 54 hpf. *E–J*, 91.7% of control embryos treated with DMSO exhibited visceral *situs solitus* (*E*). 51.4% of embryos treated with BMS453 from 32-cell to 2So displayed visceral *situs solitus* ($p < 2.0 \times 10^{-4}$; $n = 212$) (*F*), and 41.0% displayed visceral *situs inversus* ($p < 2.0 \times 10^{-4}$; $n = 212$) (*G*). 90.7% of embryos treated with BMS453 from 2So to 24 hpf showed visceral *situs solitus* ($p > 0.39$; $n = 215$) (*H*). In embryos treated with DEAB from 32-cell to 2So, 55.9% displayed visceral *situs solitus* (*I*), and 41.2% displayed visceral *situs inversus* (*J*). The *2CLIP* transgenic line with liver and pancreatic β-cells labeled with DsRed and exocrine pancreas labeled with GFP was applied in the analysis and observed at 76 hpf. *K*, percentage of embryos showed different sideness of visceral organs. *Arrowheads* mark the liver and *arrows* mark the pancreas. *p* values were calculated against control embryos treated with DMSO. *L,* left side; *R,* right side; *L/R-spawMO,* predominant distribution of *spawMO* on the left/right side; *L/R-spaw mRNA*, unilateral distribution of *spaw* mRNA on the left/right side.

laterality (Fig. 1*K*). 51.4 and 41.0% of treated embryos displayed left-sided (visceral *situs solitus*) and right-sided (visceral *situs inversus*) liver, respectively (Fig. 1, *E–G* and *K*). BMS453 treatment after 2So was ineffective on visceral laterality (Fig. 1, *H* and *K*). To confirm that these effects of BMS453 treatment are due to blockage of RA signaling, another RA antagonist DEAB, an inhibitor of RA synthase, was applied. DEAB treatment from 32-cell to 2So also resulted in randomized visceral laterality (Fig. 1, *I–K*), which recapitulated phenotypes of BMS453 treatment (Fig. 1, *F* and *G*) and could be efficiently rescued by exogenous RA (Fig. 1*K* and supplemental Table S1). These results indicate that RA signaling controls determination of visceral laterality only before 2So.

Exposure of mouse or chick embryo to exogenous RA or RA antagonist leads to aberrant heart laterality (16, 33–35). To study the role of RA signaling in controlling heart laterality as well as concordance of heart and visceral organs during LR patterning in zebrafish, effects of BMS453 treatment on heart laterality were analyzed using *Tg*(*cmlc2*:*GFP*) transgenic embryos (36). 91.1% of control embryos treated with DMSO developed normal D-loop hearts (Fig. 2, *A*, *B*, and *O*). In embryos treated with BMS453 from 32-cell to 2So, heart laterality of the majority (66.3%) remained normal at 53 h postfertilization (hpf), whereas 12.1 and 21.6% showed reversed (L-loop) and absent (midline) heart looping, respectively (Fig. 2, *C–E* and *O*). These data suggest a mild regulatory role of RA signaling before 2So in controlling heart laterality. If embryos were treated with BMS453 from 2So to 53 hpf, 39.3, 24.3, and 36.4% developed D-loop, L-loop, and midline heart, respectively (Fig. 2, *F–H* and *O*). Cardiac looping is affected by the differentiation of cardiomyocyte in addition to the laterality decisions, thus heart laterality at an earlier stage about 24 hpf was analyzed. 26.5, 21.7, and 51.8% of embryos with BMS453 treatment from 2So to 24 hpf developed left jogging, right jogging, and no jogging heart, respectively (supplemental Fig. S1). Because heart with no jogging is followed by randomized direction of looping (22), phenotypes of heart laterality at 24 hpf (supplemental Fig. S1) are in accordance with those at 53 hpf (Fig. 2, *F–H*). 87.3% of embryos treated with BMS453 from the 18-somite stage (18So) to 53 hpf displayed normal D-loop heart (Fig. 2*O* and supplemental Table S2), suggesting that RA signaling mainly controls heart laterality between 2So and 18So. Again, to confirm that these phenotypes of BMS453 treatment are due to blockage of RA signaling, DEAB was applied in the same time frames followed by examinations of heart laterality. In embryos treated with DEAB from 32-cell to 2So, 72.5, 9.2, and 18.3% developed D-loop, L-loop, and midline heart, respectively (Fig. 2, *I–K* and *O*). Those respective ratios became 87.6, 6.2, and 6.2% when RA was co-incubated for rescue (Fig. 2*O*). In contrast, if embryos were incubated with DEAB from 2So to 53

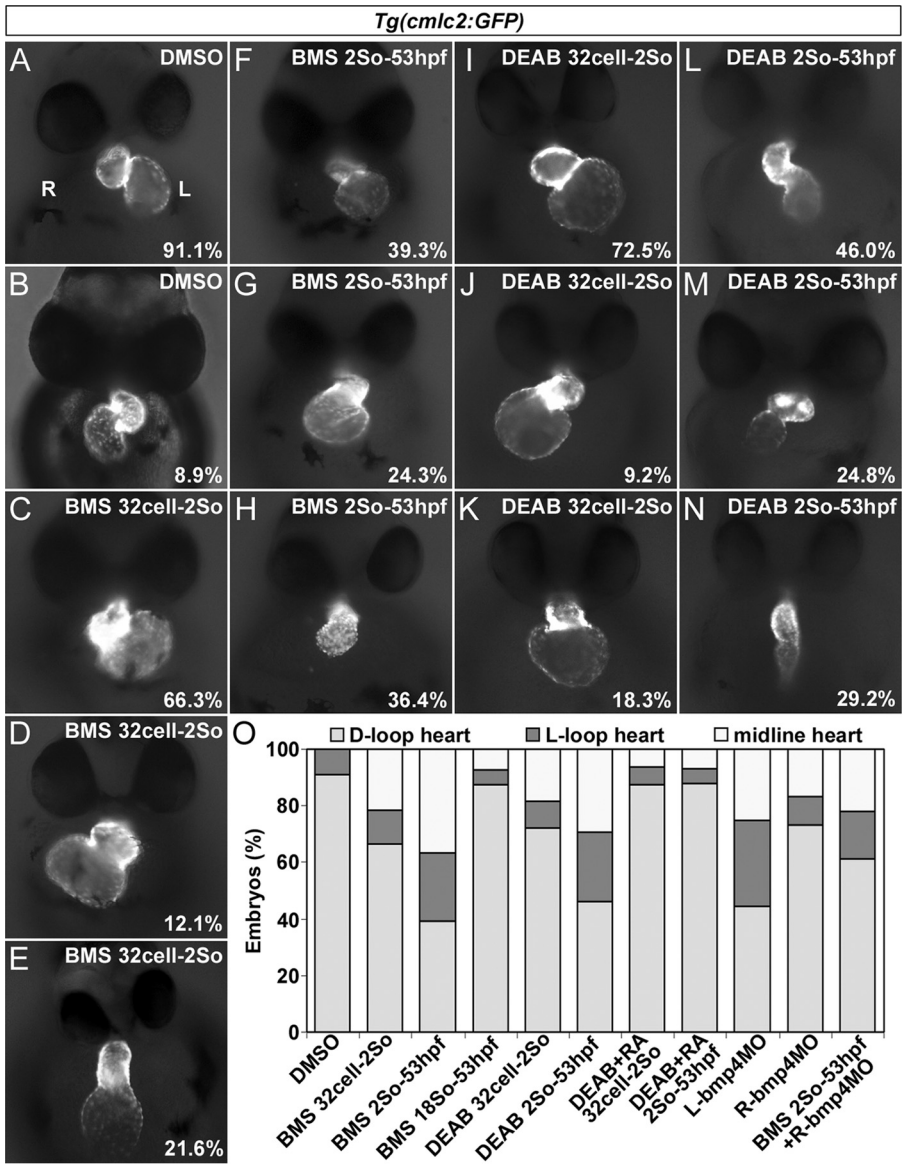

FIGURE 2. **Stage-dependent effects of RA antagonists on heart laterality.** *A* and *B*, 91.1% of control embryos treated with DMSO developed D-loop heart (*A*), whereas 8.9% developed L-loop heart (*B*). *C–E*, 66.3, 12.1, and 21.6% of embryos treated with BMS453 from 32-cell to 2So developed D-loop ($p < 0.002$; $n = 199$) (*C*), L-loop ($p > 0.40$; $n = 199$) (*D*), and midline heart ($p < 2.0 \times 10^{-4}$; $n = 199$) (*E*), respectively. *F–H*, 39.3, 24.3, and 36.4% of embryos treated with BMS453 from 2So to 53 hpf showed D-loop ($p < 2.0 \times 10^{-4}$; $n = 199$) (*F*), L-loop ($p < 0.0041$; $n = 199$) (*G*), and midline heart ($p < 3.0 \times 10^{-4}$; $n = 199$) (*H*), respectively. *I–N*, in embryos treated with DEAB from 32-cell to 2So, 72.5, 9.2, and 18.3% developed D-loop (*I*), L-loop (*J*), and midline heart (*K*), respectively. Those respective ratios became 46.0 (*L*), 24.8 (*M*), and 29.2% (*N*) when embryos were treated with DEAB from 2So to 53 hpf. *O*, percentage of embryos showed different heart laterality. *Tg*(*cmlc2*:*GFP*) transgenic embryos were observed at 53 hpf. *p* values were calculated against control embryos treated with DMSO. *L*, left side; *R*, right side; *L*/*R-bmp4MO*, predominant distribution of *bmp4MO* on the left/right side.

hpf, 46.0, 24.8, and 29.2% developed D-loop, L-loop, and midline heart, respectively (Fig. 2, *L–O*). Those respective ratios became 88.2, 4.9, and 6.9% when RA was coincubated for rescue (Fig. 2*O*). Taken together, these data indicate that the roles of RA signaling in determination of heart laterality are mild before 2So, and become much more significant after 2So.

Within embryos showing reversed visceral laterality after BMS453 treatment from 32-cell to 2So, 65.5 and 14.5% developed D-loop and L-loop heart, that is, exhibited heterotaxia and *situs inversus totalis*, respectively. Within embryos obtaining reversed heart laterality after BMS453 treatment from 2So to 53 hpf, the majority (91.3%) are with normal visceral laterality, displaying heterotaxia. These data reflect what happens in nature when heterotaxia occurs in higher frequency than *situs inversus totalis*.

Control of Visceral Laterality by RA Signaling Before 2So Is Mediated by the Left-sided Nodal Signal in the LPM—To study how RA signaling before 2So regulates visceral laterality, we first examined effects of BMS453 treatment on the left-sided *spaw* and *lefty2*. In the majority of embryos treated with BMS453 from 32-cell to 2So, both *spaw* (73.2%) and *lefty2* (83.1%) exhibited bilateral expressions (Fig. 3, *B*, *F*, *H*, and *L*, and supplemental Table S3), correlating with randomized visceral laterality (Fig. 1, *F* and *G*). In contrast, if embryos were exposed to BMS453 from 2So to 22So, *spaw* (83.6%) and *lefty2* (79.8%) kept left-sided (Fig. 3, *C*, *F*, *I*, and *L*), coinciding with

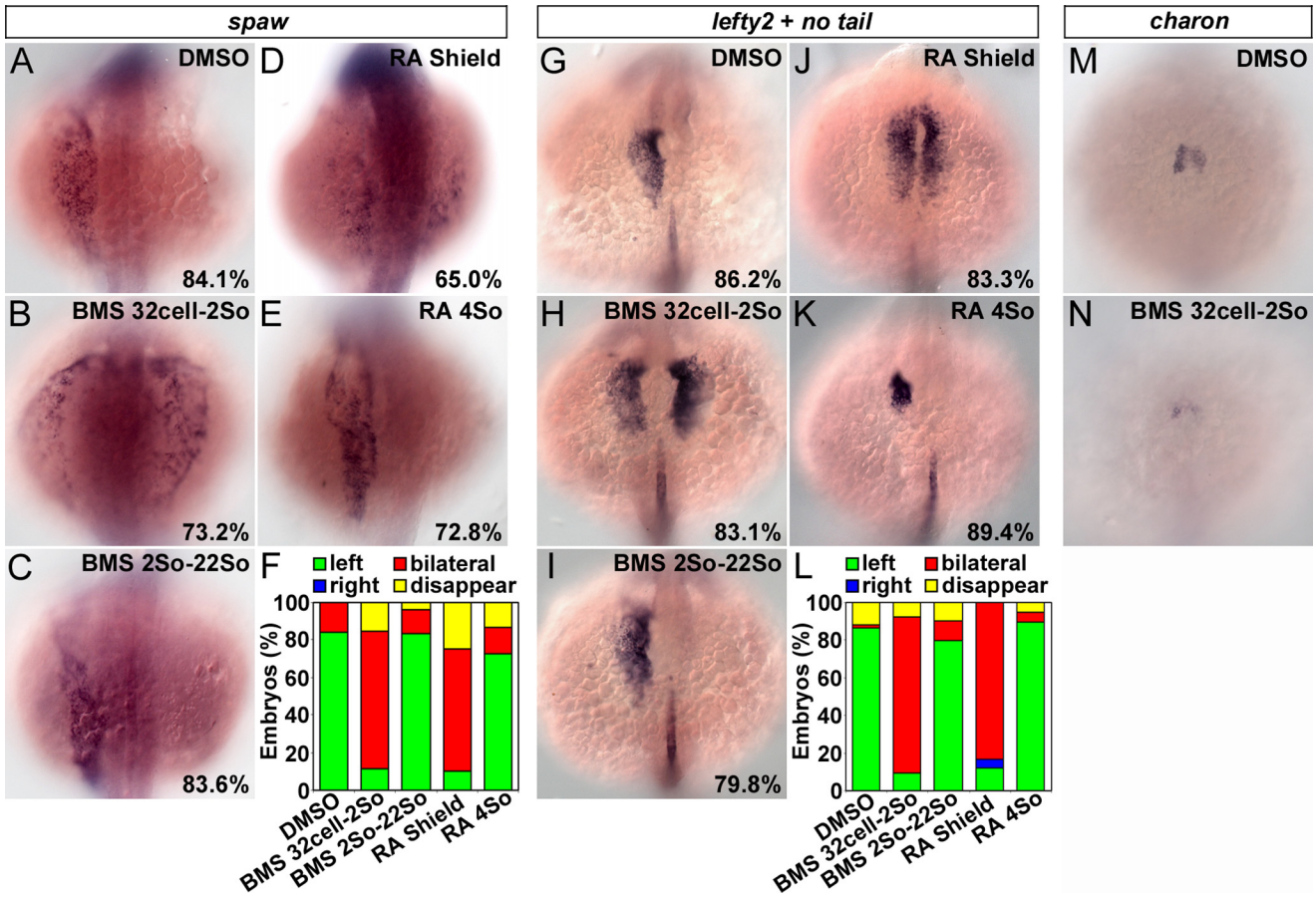

FIGURE 3. **Stage-dependent effects of RA or RA antagonist on the left-sided Nodal signal in the LPM.** 84.1 and 86.2% of DMSO-treated embryos showed left-sided *spaw* (*A*) and *lefty2* (*G*), respectively. In contrast, 73.2 and 83.1% of embryos treated with BMS453 from 32-cell to 2So exhibited bilateral expression of *spaw* ($p < 2.0 \times 10^{-5}$; $n = 71$) (*B*) and *lefty2* ($p < 3.0 \times 10^{-6}$; $n = 65$) (*H*), respectively. 83.6 and 79.8% of embryos treated with BMS453 from 2So to 22So displayed left-sided *spaw* ($p > 0.93$; $n = 73$) (*C*) and *lefty2* ($p > 0.09$; $n = 79$) (*I*), respectively. 65.0 and 83.3% of embryos treated with RA at the shield stage for 1 h and 20 min exhibited bilateral expression of *spaw* (*D*) and *lefty2* (*J*), respectively. 72.8 and 89.4% of embryos treated with RA at the 4-somite stage for 1 h and 20 min showed left-sided *spaw* (*E*) and *lefty2* (*K*), respectively. *F*, percentage of embryos showed different sideness of *spaw* expression. *L*, percentage of embryos showed different sideness of *lefty2* expression. *No tail* was applied to label the midline (*G–K*). Embryos were subjected to *in situ* hybridization at 22So and observed. *M* and *N*, expression of *charon* around KV at 10So in embryos with DMSO (*M*) or BMS453 (*N*) treatments before 2So. *p* values were calculated against control embryos treated with DMSO.

visceral *situs solitus* (Fig. 1*H*). Exogenous RA before 2So also led to a break of LR asymmetry hence bilateral *spaw* (65.0%) and *lefty2* (83.3%) in the majority of embryos (Fig. 3, *D*, *F*, *J*, and *L*). Treatment of exogenous RA after 2So was ineffective on the sideness of *spaw* (72.8%) and *lefty2* (89.4%) (Fig. 3, *E*, *F*, *K*, and *L*). *No tail* expression indicated unaffected midline formation in embryos treated with BMS453 or RA (Fig. 3, *G–K*), ruling out the possibility that bilateral *spaw* and *lefty2* resulted from aberrant midline formation. Because *charon* expression in the region of the ciliated cells is required to repress right-sided expression of *spaw* (37), decreases in *charon* expression in BMS453-treated embryos (Fig. 3, *M* and *N*) completely fit bilateral expressions of *spaw* and *lefty2*. Thus, the bilateral Nodal signal caused by BMS453 treatment is correlated with aberrant visceral laterality, proposing the involvement of the left-sided Nodal signal in mediating the control of visceral laterality by RA signaling before 2So.

To further investigate whether control of visceral laterality by RA signaling before 2So is mediated by the left-sided Nodal signal, we set up asymmetric knockdown and unilateral overexpression systems in zebrafish. A fluorescein labeled, specific antisense morpholino oligo (MO) was injected into the cell body of one cell at the 8–32-cell stage. Embryos with different distributions of MO were checked at the 64-cell as well as the shield stages, and sorted at the 10-somite stage (10So) according to fluorescein epifluorescence (supplemental Fig. S2, *A–F*). The MOs could not achieve completely unilateral distribution, but could achieve predominant distribution on one side of the zebrafish embryo. Similarly, *GFP* and target mRNAs were co-injected into the cell body of one cell at the 4–16-cell stage. Embryos with different distributions of mRNAs were sorted at the shield stage and confirmed at 10So according to GFP epifluorescence (supplemental Fig. S2, *G–M*). The mRNA was able to achieve exclusively unilateral distribution.

Embryos with *spawMO* predominantly distributed on the left side exhibited randomized visceral laterality and absent *lefty2* expression (Figs. 1*K* and 4, *A–C*), indicating the critical role of *spaw* in dictating visceral laterality. Asymmetric Spaw was re-established in BMS453-treated embryos by unilaterally predominant distributions of *spawMO*. The majority of embryos with BMS453 treatment from 32-cell to 2So and left-

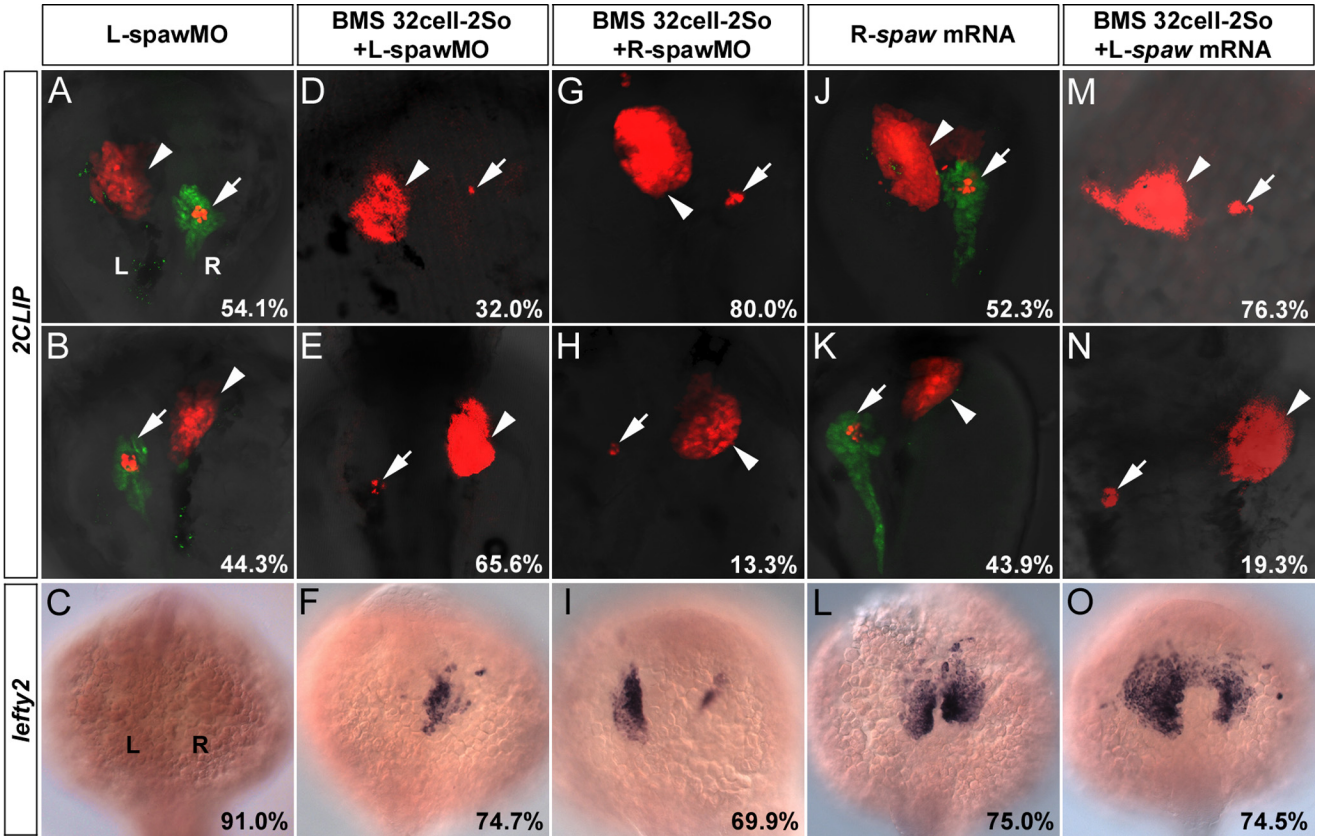

FIGURE 4. **Control of visceral laterality by RA signaling before 2So is mediated by the left-sided Nodal signal in the LPM.** *A–C,* in embryos with predominant distribution of *spawMO* on the left side, 54.1% exhibited visceral *situs solitus* ($p < 8.0 \times 10^{-4}$; $n = 122$) (*A*), 44.3% exhibited visceral *situs inversus* ($p < 4.0 \times 10^{-4}$; $n = 122$) (*B*), and 91.0% showed absent *lefty2* expression ($p < 9.0 \times 10^{-5}$; $n = 78$) (*C*). *D–F*, in embryos with both BMS453 treatment from 32-cell to 2So and predominant distribution of *spawMO* on the left side, 32.0% exhibited visceral *situs solitus* ($p < 7.0 \times 10^{-5}$; $n = 125$) (*D*), 65.6% exhibited visceral *situs inversus* ($p < 2.0 \times 10^{-5}$; $n = 125$) (*E*), and 74.7% showed predominant *lefty2* expression on the right side ($p < 7.0 \times 10^{-6}$; $n = 91$) (*F*). *G–I*, in embryos with both BMS453 treatment from 32-cell to 2So and predominant distribution of *spawMO* on the *right side*, 80.0% exhibited visceral *situs solitus* ($p < 0.0017$; $n = 135$) (*G*), 13.3% exhibited visceral *situs inversus* ($p < 5.0 \times 10^{-4}$; $n = 135$) (*H*), and 69.9% showed predominant *lefty2* expression on the left side ($p < 9.0 \times 10^{-5}$; $n = 103$) (*I*). *p* values in *G–I* were calculated against embryos treated with BMS453 from 32-cell to 2So. *J–L*, in embryos with unilateral distribution of exogenous *spaw* mRNA on the right side, 52.3% exhibited visceral *situs solitus* ($p < 5.0 \times 10^{-4}$; $n = 130$) (*J*), 43.9% exhibited visceral *situs inversus* ($p < 6.0 \times 10^{-5}$; $n = 130$) (*K*), and 75.0% showed bilateral *lefty2* expression ($p < 4.0 \times 10^{-6}$; $n = 88$) (*L*). Note that development of exocrine pancreas was unaffected (*J and K*). *M–O*, in embryos with both BMS453 treatment from 32-cell to 2So and unilateral distribution of exogenous *spaw* mRNA on the left side, 76.3% exhibited visceral *situs solitus* ($p < 5.0 \times 10^{-4}$; $n = 207$) (*M*), 19.3% exhibited visceral *situs inversus* ($p < 0.0028$; $n = 207$) (*N*), and 74.5% showed asymmetric *lefty2* with stronger expression on the left side ($p < 5.0 \times 10^{-5}$; $n = 106$) (*O*). *p* values in *M–O* were calculated against embryos treated with BMS453 from 32-cell to 2So. *Arrowheads* mark the liver and *arrows* mark the pancreas. *2CLIP* transgenic embryos were observed at 76 hpf. Embryos were subjected to *in situ* hybridization at 22So and observed. Unless specifically mentioned, *p* values were calculated against control embryos treated with DMSO. *L*, left side; *R*, right side; *L/R-spawMO*, predominant distribution of *spawMO* on the left/right side; *L/R-spaw mRNA*, unilateral distribution of *spaw* mRNA on the left/right side.

sided enrichment of *spawMO* became visceral *situs inversus* (65.6%) (Figs. 1*K* and 4, *D* and *E*), and predominantly expressed *lefty2* on the right side (74.7%) (Fig. 4*F*). In contrast, the majority of embryos with BMS453 treatment from 32-cell to 2So and right-sided enrichment of *spawMO* exhibited visceral *situs solitus* (80.0%) (Figs. 1*K* and 4, *G* and *H*) and predominant expression of *lefty2* on the left side (69.9%) (Fig. 4*I*), rescuing randomized visceral laterality and bilateral *lefty2* caused by BMS453 (Figs. 1, *F*, *G*, and *K*, and 3*H*). Restoration of Spaw asymmetry through unilateral depletion with *spawMO* in BMS453-treated embryos dictates visceral laterality, indicating that the left-sided Nodal signal mediates the control of visceral laterality by RA signaling before 2So.

We further studied whether establishment of Spaw asymmetry through unilateral distribution of exogeous *spaw* mRNA is sufficient to dictate visceral laterality or not. 82.0% of embryos with exclusive distribution of exogenous *spaw* mRNA on the left side displayed visceral *situs solitus* (Fig. 1*K*). In embryos with exogenous *spaw* mRNA unilateral on the right side, visceral laterality was randomized without affecting exocrine pancreas differentiation and bilateral *lefty2* was induced (Figs. 1*K* and 4, *J–L*). Embryos with BMS453 treatment from 32-cell to 2So and left-sided distribution of exogenous *spaw* mRNA accumulated more *spaw* transcripts on the left than on the right side. 76.3 and 19.3% of these embryos exhibited visceral *situs solitus* and *situs inversus*, respectively (Figs. 1*K* and 4, *M* and *N*). In addition, asymmetric *lefty2* with stronger expression on the left side was observed (Fig. 4*O*). Establishment of *spaw* asymmetry is sufficient to rescue randomized visceral laterality caused by BMS453, again demonstrating the critical role of the left-sided Nodal signal in mediating control of visceral laterality by RA signaling before 2So.

In zebrafish, ciliogenesis in KV is required for establishment of the left-sided Nodal signal in the LPM (1–3). Thus, involvements of RA signaling before 2So in the formation of KV and ciliogenesis were analyzed. At 10So, although KV formation

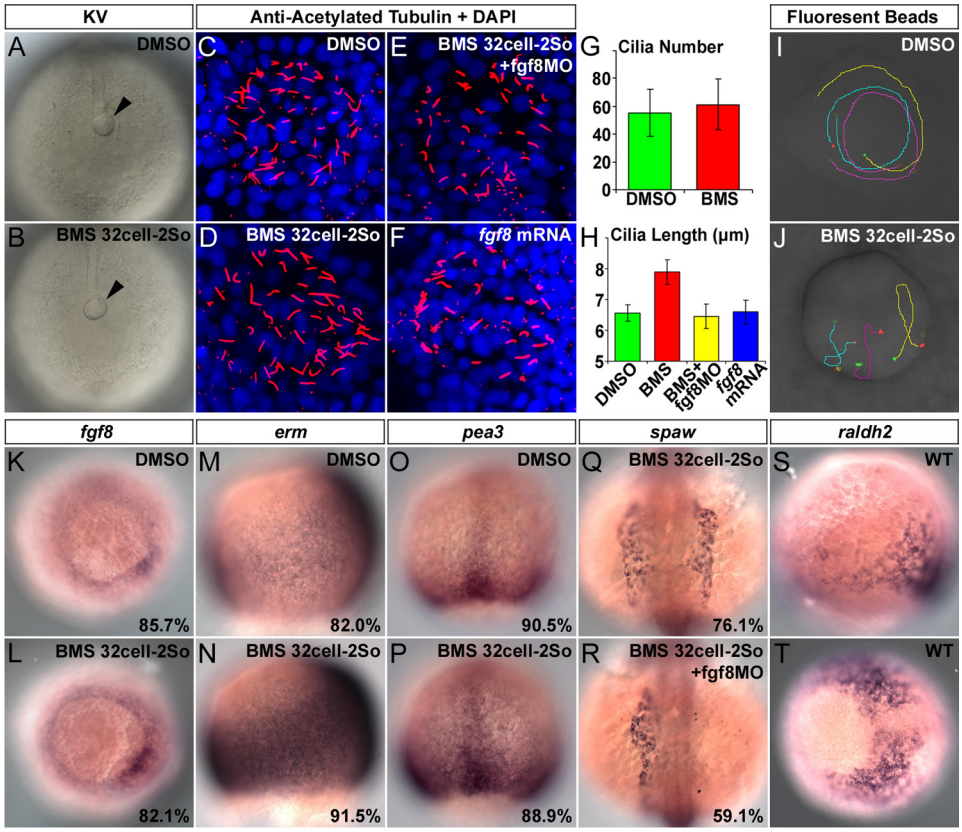

FIGURE 5. **RA signaling before 2So regulates cilia length and KV fluid flow, in which Fgf8 is required.** *A* and *B*, in contrast to control embryos treated with DMSO (*A*), the formation of KV was unaffected in embryos treated with BMS453 from 32-cell to 2So (*B*). *Arrowheads* mark the KV. *C–F*, in contrast to control embryos treated with DMSO (*C*), embryos treated with BMS453 from 32-cell to 2So displayed increased cilia length in KV ($p < 0.0015$) (*D*), which was rescued by the injection of *fgf8MO* (*E*). Overexpression of *fgf8* mRNA alone was not sufficient to lead to increases in cilia length (*F*). *G*, the number of cilia between DMSO- and BMS453-treated embryos showed no obvious difference. *H*, in contrast to control embryos treated with DMSO, cilia lengths were increased in embryos treated with BMS453 from 32-cell to 2So ($p < 0.0015$), but not in embryos with both BMS453 treatment and *fgf8MO* injection ($p > 0.88$). Cilia length in embryos with *fgf8* mRNA injection also showed no obvious difference ($p > 0.63$). *I* and *J*, in control embryos treated with DMSO, fluorescent beads had a persistent counterclockwise directional flow (*I*). Movement of beads in embryos with BMS453 treatment before 2So became non-directional (*J*). *Green spots*, *red spots*, and *curves* mark the start points, end points, and tracks of beads movements, respectively. *K–P*, in contrast to control embryos treated with DMSO (*K, M, O*), transcriptions of *fgf8* (*L*) at the marginal zone as well as its downstream targets *erm* (*N*) and *pea3* (*P*) were enhanced in embryos treated with BMS453 from 32-cell to 80% epiboly. Embryos were viewed from the bottom (*K* and *L*), the lateral (*M* and *N*), and the dorsal (*O* and *P*) sides. *Q* and *R*, low concentration (60 μM) of *fgf8MO* (*R*) efficiently rescued bilateral *spaw* expression caused by BMS453 treatment before 2So (*Q*). *S* and *T*, lateral (*S*) and bottom (*T*) view of *raldh2* expression at 80%E with the dorsal side to the right. *p* values were calculated against control embryos treated with DMSO.

and the number of cilia in it exhibited no obvious difference (Fig. 5, *A–D* and *G*), increases in cilia length were observed in embryos exposed to BMS453 from 32-cell to 2So (Fig. 5, *C*, *D*, and *H*). To assess whether cilia-driven directional fluid flow in KV was altered in BMS453-treated embryos, we tracked movements of fluorescent beads injected into the lumen of KV (2). Fluorescent beads in control embryos had a persistent counterclockwise directional flow (Fig. 5*I* and supplemental Movie S1). In contrast, movements of beads in embryos treated with BMS453 before 2So became non-directional (Fig. 5*J* and supplemental Movie S2). FGF signaling during gastrulation regulates cilia length in KV and RA signaling in many contexts opposes FGF signaling, for instance, during body axis extension, spinal cord differentiation, and limb bud development (4, 38–41). Therefore, we analyzed whether FGF signaling mediates or is correlated with the increases in cilia length caused by BMS453. The increased cilia length in BMS453-treated embryos was rescued by *fgf8MO* (Fig. 5, *E* and *H*), indicating that *fgf8* is required to mediate the regulation of cilia length by RA signaling. Overexpression of *fgf8* alone was not sufficient to lead to increases in cilia length (4) (Fig. 5, *F* and *H*). However, in BMS453-treated embryos, enhanced *fgf8* transcription at the marginal zone was concomitant with the increases in cilia length at the 80% epiboly stage (80%E) (Fig. 5, *C*, *D*, *K*, and *L*, and supplemental Fig. S3 and Table S4). This implied that Fgf8 may require co-factors to synergically regulate cilia length in KV downstream of RA signaling. Up-regulation of FGF signaling in BMS453-treated embryos was also confirmed by enhanced transcriptions of FGF targets, *erm* and *pea3*, at 80%E (Fig. 5, *M–P*, and supplemental Fig. S3). Furthermore, low concentrations of *fgf8MO* efficiently rescued bilateral *spaw* and partially rescued the decreases in *charon* expression in BMS453-treated embryos (Fig. 5, *Q* and *R*, and supplemental Fig. S4). All these results demonstrate that RA signaling before 2So regulates cilia length as well as KV fluid flow, and Fgf8 is required for this regulation.

To find the source of RA that regulates ciliogenesis and visceral laterality before 2So, expression patterns of the major RA synthesis enzyme *retinaldehyde dehydrogenase 2* (*raldh2*) were analyzed at 80%E (Fig. 5, *S* and *T*). *raldh2* was expressed in the dorsal half of the marginal zone, around the dorsal forerunner cells and partially overlapping with the *fgf8* expression. This

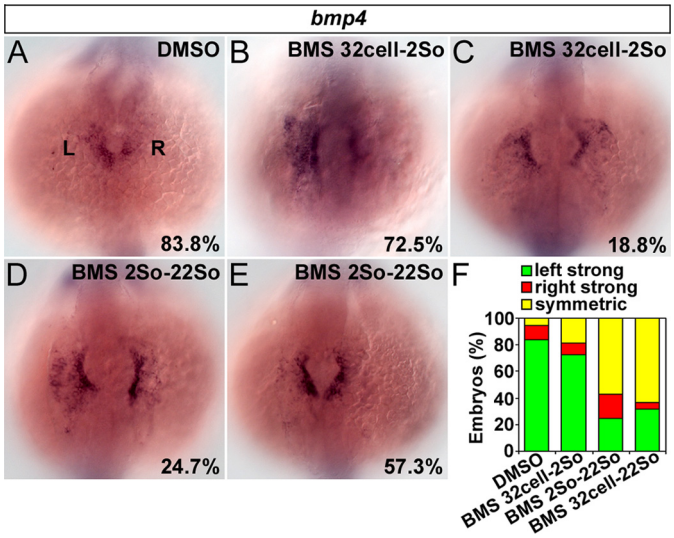

FIGURE 6. **Stage-dependent effects of RA antagonist on cardiac *bmp4* asymmetry.** *A*, 83.8% of control embryos treated with DMSO showed stronger cardiac *bmp4* on the left than on the right side. *B* and *C*, in contrast, 72.5 and 18.8% of embryos treated with BMS453 from 32-cell to 2So exhibited stronger cardiac *bmp4* on the left side ($p < 0.02$; $n = 80$) (*B*) and symmetric cardiac *bmp4* ($p < 0.007$; $n = 80$) (*C*), respectively. *D* and *E*, in embryos treated with BMS453 from 2So to 22So, 24.7 and 57.3% showed stronger *bmp4* in the left cardiac field ($p < 2.0 \times 10^{-7}$; $n = 89$) (*D*) and symmetric *bmp4* ($p < 5.0 \times 10^{-5}$; $n = 89$) (*E*), respectively. *F*, percentage of embryos showed different cardiac *bmp4* asymmetries. Embryos were applied to *in situ* hybridization at 22So and observed. *p* values were calculated against control embryos treated with DMSO.

dorsal half of the marginal zone is the possible source of RA activity before 2So that regulates *fgf8* transcription and ciliogenesis.

Control of Heart Laterality by RA Signaling After 2So Is Mediated by Asymmetric bmp4 in the Cardiac Field—Because sideness of *spaw* and *lefty2* was unaffected by BMS453 treatment after 2So (Fig. 3, *C* and *I*), the left-sided Nodal signal could not mediate the control of heart laterality by RA signaling after 2So. To study whether asymmetric *bmp4* in the cardiac field within the LPM acts as the mediator, effects of BMS453 on *bmp4* were analyzed. 83.8% of control embryos showed stronger cardiac *bmp4* on the left than on the right side at 22So (Fig. 6, *A* and *F*, and supplemental Fig. S5*A*). In embryos exposed to BMS453 from 32-cell to 2So, 72.5 and 18.8% exhibited stronger *bmp4* in the left cardiac field and symmetric cardiac *bmp4*, respectively (Fig. 6, *B*, *C*, and *F*, and supplemental Fig. S5*B*). If embryos were treated with BMS453 from 2So to 22So, ratios of embryo with stronger *bmp4* on the left side and symmetric *bmp4* became 24.7 and 57.3%, respectively (Fig. 6, *D*–*F*, and supplemental Fig. S5*C*). These respective ratios became 31.6 and 63.1% if embryos were incubated with BMS453 from 32-cell to 22So, close to those of treatments from 2So to 22So (Fig. 6*F*). Disturbed cardiac *bmp4* asymmetry caused by BMS453 treatment after 2So was correlated with aberrant heart laterality, proposing the involvement of cardiac *bmp4* in mediating the control of heart laterality by RA signaling after 2So.

Asymmetric knockdown of Bmp4 was achieved using a fluorescein-labeled *bmp4MO*. In embryos with *bmp4MO* predominantly distributed on the left side, cardiac Bmp4 asymmetry was perturbed. 44.4, 30.6, and 25.0% showed D-loop, L-loop, and midline heart, respectively (Fig. 2*O*). In embryos with bmp4MO predominantly distributed on the right side, cardiac bmp4 asymmetry remained so that 73.3% of embryos displayed the normal D-loop heart (Fig. 2*O*). These data illustrate the significance of Bmp4 asymmetry in the control of heart laterality. To investigate whether determination of heart laterality by RA signaling after 2So is mediated by the asymmetric cardiac *bmp4*, Bmp4 asymmetry was re-established in BMS453-treated embryos by a predominant distribution of *bmp4MO* on the right side (supplemental Table S5). In embryos with BMS453 treatment from 2So to 22So and right-sided enrichment of *bmp4MO*, ratios of D-loop, L-loop, and midline heart became 61.4, 16.5, and 22.1%, respectively (Figs. 2*O* and 7, *A*–*C*) In embryos with BMS453 treatment from 2So to 22So but without *bmp4MO*, those respective ratios were 39.3, 24.3, and 36.4% (Fig. 2, *F*–*H* and *O*). Re-establishment of bmp4 asymmetry rescues aberrant heart laterality caused by BMS453, indicating that cardiac Bmp4 mediates the control of heart laterality by RA signaling after 2So.

To find the source of RA that regulates heart laterality after 2So, expression patterns of *raldh2* were analyzed. Besides the somatic mesoderm, *raldh2* was found to express in the anterior LPM at 10So, slightly asymmetric with stronger expression on the left side and partially overlapping with precardiac mesoderm (42, 43) (Fig. 7, *D*–*G*). This slightly asymmetric expression of *raldh2* initiated at 1–2So and became evident from 3 to 4So forward (Fig. 7, *H* and *I*). These temporal patterns explain why RA signaling controls heart laterality mainly after 2So. Asymmetry of *raldh2* was unaffected in Spaw morphant (Fig. 7*J*), indicating that the establishment of *raldh2* asymmetry in the anterior LPM is independent of the left-sided Nodal signal. These results suggest a possible source of RA important for the control of heart laterality, which locates asymmetrically in the anterior LPM from 1 to 2So forward.

DISCUSSION

In summary, our results suggest that RA signaling regulates LR patterning of organs at two stages in zebrafish. Before 2So, RA signaling is critical for setting up the left-sided Nodal signal through regulation of cilia length and KV fluid flow. *fgf8* is required to mediate this regulation. The left-sided Nodal signal is the key dictator of visceral laterality so that RA signaling controls visceral laterality before 2So. Roles of RA signaling in the determination of heart laterality are mild before 2So, and become much more significant after 2So through regulation of cardiac *bmp4* asymmetry. Although previous studies have reported that visceral and heart laterality is sometimes uncoordinated so that their asymmetries may need concordance (21, 24), our study first identifies RA signaling as the key signaling pathway that sequentially controls and coordinates visceral and heart laterality.

Titrations for the cut-off time at the shield, 80%E, bud, 2So, and 4So have identified the significance of 2So (data not shown). Theoretically, on one hand, formation of KV and cilia are initially observed at 3–4So (2) (data not shown). Thus, RA signaling should be functional to regulate ciliogenesis before that. This point was proven by the unaffected sideness of *spaw* and *lefty2* after RA treatment at 4So (Fig. 3, *E* and *K*). On the other hand, asymmetric expression of *raldh2* in the anterior

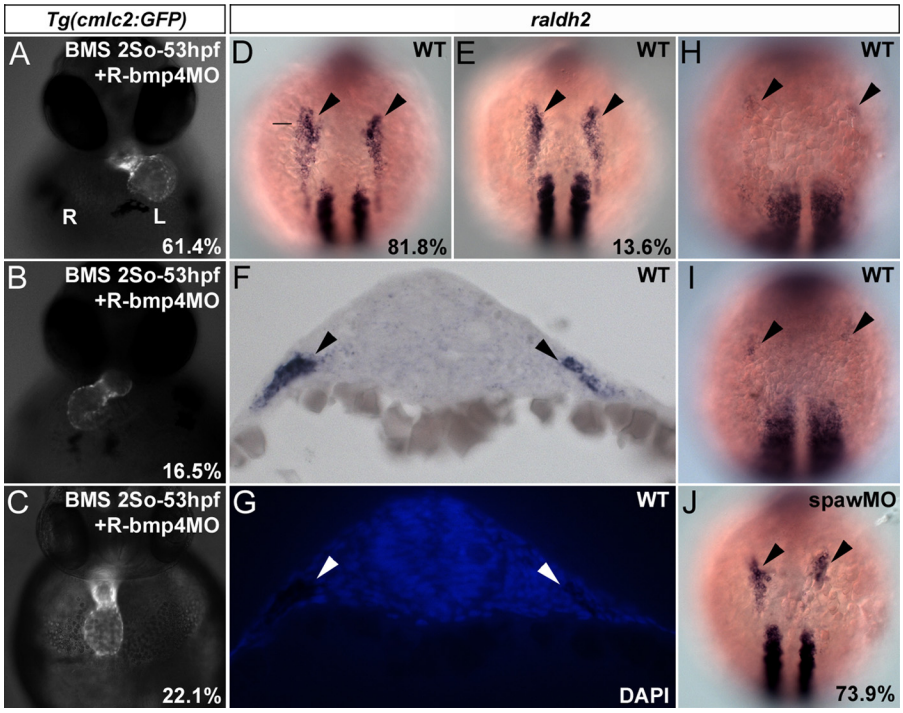

FIGURE 7. **Control of heart laterality by later RA signaling after 2So is mediated by asymmetric *bmp4*.** *A–C*, in embryos with both BMS453 treatment from 2So to 53 hpf and predominant distribution of *bmp4MO* on the right side, 61.4, 16.5, and 22.1% developed D-loop ($p < 0.0065$; $n = 127$) (*A*), L-loop ($p < 0.0021$; $n = 127$) (*B*), and midline ($p < 0.02$; $n = 127$) (*C*) heart, respectively. Living *Tg*(*cmlc2*:*GFP*) transgenic embryos were observed at 53 hpf. *p* values were calculated against embryos treated with BMS453 from 2So to 53 hpf. *D* and *E*, in wild type embryos at 10So, 81.8% exhibited slightly asymmetric *raldh2* with stronger expression on the left side in the anterior LPM (*D*), whereas 13.6% showed symmetric *raldh2* expression (*E*). The *line* marks the position of the section plane shown in *F* and *G*. *F*, sections illustrated asymmetric expression of *raldh2* in the anterior LPM at 10So. *G*, *in situ* image of the section was overlaid with DAPI counterstaining. *H* and *I*, slightly asymmetric expression of *raldh2* in the anterior LPM initiated at 1–2So (*H*) and became evident at 3–4So (*I*). *J*, 73.9% of *spaw* morphants showed slightly asymmetric *raldh2* with stronger transcription on the left side in the anterior LPM. *Arrowheads* mark the transcription of *raldh2* in the anterior LPM. *WT*, wild type.

LPM initiates at 1–2So (Fig. 7H). Therefore, control of cardiac *bmp4* asymmetry by RA signaling is enabled only after that. These two aspects fit our titration results and supply possible explanations why 2So becomes a critical cut-off time.

Discrepancy between treatments of RA antagonist and *raldh2* mutation have been previously reported in mice and discussed in two papers published by the same laboratory (16, 44). One of the papers showed disturbed sideness of *nodal* and *lefty* in mouse embryos treated with RA antagonist (16), whereas the second exhibited unaffected sideness of *nodal* and *pitx2* in *raldh2*$^{-/-}$ mouse mutant (44). This discrepancy could also exist in zebrafish (45), and be explained by the following four possible reasons. First, other RA synthesis enzymes like Raldh1, Raldh3, and Raldh4 play redundant roles in the *raldh2* mutant or morphant. But BMS453, a pan-retinoic acid receptor antagonist, was able to achieve a more complete inhibition of RA signaling. Second, maternal Raldh2 protein or mRNA plays an important role in setting up the left-sided Nodal signal. Actually, maternal transcripts of *raldh2*, *raldh3*, and *raldh4* have all been reported in zebrafish (46, 47). From this aspect, BMS453 or DEAB could also achieve a more complete inhibition of RA signaling. Third, RA antagonists result in stronger phenotypes than *raldh2* mutation, which has been reported in two *raldh2* mutant alleles in zebrafish (46). Fourth, *raldh2* morpholino only represents a knockdown of Raldh2. A certain percentage of Raldh2 activity may still exist. Therefore, differences between chemical inhibitors and genetic inactivation have been sufficiently interpreted.

Although RA signaling is required in more than one aspect of visceral organ development, such as pancreas differentiation and visceral laterality (29) (Fig. 1), our results demonstrate that LR effects of BMS453 treatment on heart and visceral organs are specific other than indirect. First, both predominantly right-sided distribution of *spawMO* and unilaterally left-sided distribution of exogenous *spaw* mRNA specifically rescued randomization of visceral laterality but not defective pancreas differentiation caused by BMS453 (Figs. 1, *F* and *G*, and 4, *G*, *H*, *M*, and *N*). Second, both BMS453 treatments before and after 2So caused no obvious early phenotype up to 25 hpf when laterality decisions have already been made (supplemental Fig. S6), ruling out the possibility that the LR phenotypes are indirect effects of earlier phenotypes. Third, defective laterality of heart and visceral organs caused by DEAB could be efficiently rescued by exogenous RA (Figs. 1*K* and 2*O*). Fourth, BMS453 or DEAB treatments led to differentiation phenotypes of cardiac progenitors before 2So (Fig. 2, *C–E* and *I–K*) and defective heart laterality mainly after 2So (Fig. 2, *F–H* and *L–N*). They are temporally separated.

BMS453 and DEAB lead to similar laterality phenotypes at the same stage, which confirms that the phenotypes are due to blockage of RA signaling. However, BMS453 appears to be a stronger RA antagonist than DEAB. First, BMS453 treatment from 32-cell to 2So leads to a complete absence of exocrine pancreas as well as dramatic reduction of β-cells (Figs. 1, *F* and *G*, and 4, *D–H*, *M*, and *N*). In contrast, a residual of exocrine pancreas and mild reduction of β-cells were observed in the

majority of embryos treated with DEAB (Fig. 1, *I* and *J*). Second, ratios of defective heart laterality were a little higher in embryos treated with BMS453 than DEAB (Fig. 2, *C–O*). These differences between BMS453 and DEAB can be explained by different mechanisms of how these chemicals work. BMS453, whose inhibitory effects cannot be rescued by exogenous RA, is a pan-retinoic acid receptor antagonist. DEAB is an inhibitor of RA synthase, and its effects can be efficiently rescued by exogenous RA.

Both *fgf8* knockdown and overexpression resulted in decreases in *charon* transcription around KV (5) (supplemental Fig. S4, *A–C*), indicating that a certain Fgf8 concentration is necessary for *charon* activation. This also explains why decreases in *charon* transcription after BMS453 treatment were exacerbated by a high concentration of *fgf8MO*, but partially rescued by a low concentration of *fgf8MO* (supplemental Fig. S4, *D–F*).

Increases in heart size and expansion of cardiac *bmp4* expression caused by BMS453 or DEAB treatment from 32-cell to 2So (Figs. 2, *C–E* and *I–K*, and 6*B*) should result from increases in cell number of cardiac progenitors (48, 49). Because cardiac looping is not only controlled by the laterality decisions but also affected by the differentiation of cardiomyocyte, the mild role of RA signaling before 2So in regulating heart laterality could be a result of increases in cardiac progenitors. It is also possible that RA signaling before 2So mildly regulates heart laterality through the left-sided Nodal signal or other unknown mechanisms. At 22So, the asymmetric, bilateral cardiac primordia have fused in zebrafish. In embryos treated with BMS453, although there is no delay in embryonic development (supplemental Fig. S5), the bilateral cardiac primoridia have not yet fused (Fig. 6, *B–E*). This delay in fusion of cardiac primordia could be a result of perturbed heart laterality, or a result of increases in cardiac progenitors, or an independent effect.

Knockdown of Bmp4 in the dorsal forerunner cells or ectopic expression of noggin3 lead to bilateral expression of *spaw* (21). However, except for unaffected formation of KV in *bmp4* morphant, mechanisms underlying regulation of the left-sided Nodal signal by *bmp4* remain unknown. Expression patterns during gastrulation (only in the ventral region and prechordal plate) precludes Bmp4 as an upstream factor of RA and FGF signaling in regulating ciliogenesis. Expression of *bmp4* around KV at 10So remained unaffected in embryos treated with BMS453 from 32-cell to 2So (supplemental Fig. S7), excluding bmp4 as a downstream factor of RA signaling. Therefore, unlike RA and FGF signaling that regulate cilia length, bmp4 most probably plays parts in other aspects of ciliogenesis or even independent of ciliogenesis.

Both blockage of RA signaling and exogenous RA represent disturbance of LR asymmetry under the control of RA signaling, which could explain why both BMS453 and RA treatments do lead to similar effects on the left-sided Nodal signal (34) (Fig. 3). It has been reported that *spaw* morphant displays disturbed cardiac *bmp4* asymmetry as well as defective heart laterality (11, 21), and reversed asymmetry of *lefty2* is accompanied by reversed heart laterality (50). However, it is likely that if the left-sided Nodal is present, repression of the Nodal signal in the right LPM is less significant for cardiac *bmp4* asymmetry and heart laterality (Figs. 2*C*, 3, *B* and *H*, and 6*B*). In other words, the Nodal asymmetry could be inconsistent with cardiac *bmp4* asymmetry and heart laterality. This inconsistency has been previously reported both in mice and zebrafish (44, 51). One reference showed normal sideness of Nodal signal in the LPM of *raldh2*$^{-/-}$ mouse, but its heart laterality was defective (44). The other showed bilateral expression of *spaw* in *aei*$^{-/-}$ zebrafish mutant, but its heart laterality remains unaffected (51). The concomitance of asymmetrically normal *spaw* and *lefty2*, correct visceral laterality, disturbed cardiac *bmp4*, and aberrant heart laterality (Figs. 1*H*, 2, *F–H*, 3, *C* and *I*, and 6*E*) indicates that cardiac *bmp4* asymmetry and heart laterality are not under the direct control of the left-sided Nodal signal, and cardiac *bmp4* is insignificant to the determination of visceral laterality. Furthermore, from our results, although LR asymmetry is phenotypically evident first in the heart, its laterality determination even takes place later than that of visceral organs.

Taken together, our data suggest that RA signaling regulates LR patterning of organs at two stages, shedding new light on how concordance of visceral and heart laterality is achieved. Before 2So, RA signaling regulates cilia length and directional fluid flow in KV by the mediation of *fgf8*. This is critical for setting up the left-sided Nodal signal that dictates visceral laterality. From 2So on, because a possible new RA resource appears in the anterior LPM, the mild regulatory role of RA signaling before 2So in controlling heart laterality becomes much more significant after 2So through asymmetric cardiac *bmp4*.

Acknowledgments—We thank Dr. Yonglong Chen for BMS453, Dr. Stephen W. Wilson, Dr. Jeroen Bakkers, and Dr. Wolfgang Driever for plasmids, and Dr. Didier Y. R. Stainier for fish lines.

REFERENCES

1. Essner, J. J., Vogan, K. J., Wagner, M. K., Tabin, C. J., Yost, H. J., and Brueckner, M. (2002) *Nature* **418,** 37–38
2. Essner, J. J., Amack, J. D., Nyholm, M. K., Harris, E. B., and Yost, H. J. (2005) *Development* **132,** 1247–1260
3. Yost, H. J. (2003) *Curr. Biol.* **13,** R808–R809
4. Neugebauer, J. M., Amack, J. D., Peterson, A. G., Bisgrove, B. W., and Yost, H. J. (2009) *Nature* **458,** 651–654
5. Hong, S. K., and Dawid, I. B. (2009) *Proc. Natl. Acad. Sci. U.S.A.* **106,** 2230–2235
6. Raya, A., and Izpisúa Belmonte, J. C. (2006) *Nat. Rev. Genet.* **7,** 283–293
7. Levin, M., Johnson, R. L., Stern, C. D., Kuehn, M., and Tabin, C. (1995) *Cell* **82,** 803–814
8. Collignon, J., Varlet, I., and Robertson, E. J. (1996) *Nature* **381,** 155–158
9. Lowe, L. A., Supp, D. M., Sampath, K., Yokoyama, T., Wright, C. V., Potter, S. S., Overbeek, P., and Kuehn, M. R. (1996) *Nature* **381,** 158–161
10. Lustig, K. D., Kroll, K., Sun, E., Ramos, R., Elmendorf, H., and Kirschner, M. W. (1996) *Development* **122,** 3275–3282
11. Long, S., Ahmad, N., and Rebagliati, M. (2003) *Development* **130,** 2303–2316
12. Meno, C., Ito, Y., Saijoh, Y., Matsuda, Y., Tashiro, K., Kuhara, S., and Hamada, H. (1997) *Genes Cells* **2,** 513–524
13. Meno, C., Saijoh, Y., Fujii, H., Ikeda, M., Yokoyama, T., Yokoyama, M., Toyoda, Y., and Hamada, H. (1996) *Nature* **381,** 151–155
14. Piedra, M. E., Icardo, J. M., Albajar, M., Rodriguez-Rey, J. C., and Ros, M. A. (1998) *Cell* **94,** 319–324
15. Ryan, A. K., Blumberg, B., Rodriguez-Esteban, C., Yonei-Tamura, S., Ta-

mura, K., Tsukui, T., de la Peña, J., Sabbagh, W., Greenwald, J., Choe, S., Norris, D. P., Robertson, E. J., Evans, R. M., Rosenfeld, M. G., and Izpisúa Belmonte, J. C. (1998) *Nature* **394,** 545–551
16. Chazaud, C., Chambon, P., and Dollé, P. (1999) *Development* **126,** 2589–2596
17. Ramsdell, A. F., and Yost, H. J. (1999) *Development* **126,** 5195–5205
18. Rodríguez Esteban, C., Capdevila, J., Economides, A. N., Pascual, J., Ortiz, A., and Izpisúa Belmonte, J. C. (1999) *Nature* **401,** 243–251
19. Yokouchi, Y., Vogan, K. J., Pearse, R. V., 2nd, and Tabin, C. J. (1999) *Cell* **98,** 573–583
20. Chang, H., Zwijsen, A., Vogel, H., Huylebroeck, D., and Matzuk, M. M. (2000) *Dev. Biol.* **219,** 71–78
21. Chocron, S., Verhoeven, M. C., Rentzsch, F., Hammerschmidt, M., and Bakkers, J. (2007) *Dev. Biol.* **305,** 577–588
22. Chen, J. N., van Eeden, F. J., Warren, K. S., Chin, A., Nüsslein-Volhard, C., Haffter, P., and Fishman, M. C. (1997) *Development* **124,** 4373–4382
23. Smith, K. A., Chocron, S., von der Hardt, S., de Pater, E., Soufan, A., Bussmann, J., Schulte-Merker, S., Hammerschmidt, M., and Bakkers, J. (2008) *Dev. Cell* **14,** 287–297
24. Schilling, T. F., Concordet, J. P., and Ingham, P. W. (1999) *Dev. Biol.* **210,** 277–287
25. Albertson, R. C., and Yelick, P. C. (2005) *Dev. Biol.* **283,** 310–321
26. Liu, X., Huang, S., Ma, J., Li, C., Zhang, Y., and Luo, L. (2009) *J. Cell Biol.* **184,** 805–815
27. Carl, M., Bianco, I. H., Bajoghli, B., Aghaallaei, N., Czerny, T., and Wilson, S. W. (2007) *Neuron* **55,** 393–405
28. Ellertsdottir, E., Ganz, J., Dürr, K., Loges, N., Biemar, F., Seifert, F., Ettl, A. K., Kramer-Zucker, A. K., Nitschke, R., and Driever, W. (2006) *Dev. Dyn.* **235,** 1794–1808
29. Jiang, Z., Song, J., Qi, F., Xiao, A., An, X., Liu, N. A., Zhu, Z., Zhang, B., and Lin, S. (2008) *PLoS Biol.* **6,** e293
30. Field, H. A., Ober, E. A., Roeser, T., and Stainier, D. Y. R. (2003) *Dev. Biol.* **253,** 279–290
31. Schulze, G. E., Clay, R. J., Mezza, L. E., Bregman, C. L., Buroker, R. A., and Frantz, J. D. (2001) *Toxicol. Sci.* **59,** 297–308
32. Anderson, R. M., Bosch, J. A., Goll, M. G., Hesselson, D., Dong, P. D., Shin, D., Chi, N. C., Shin, C. H., Schlegel, A., Halpern, M., and Stainier, D. Y. (2009) *Dev. Biol.* **334,** 213–223
33. Smith, S. M., Dickman, E. D., Thompson, R. P., Sinning, A. R., Wunsch, A. M., and Markwald, R. R. (1997) *Dev. Biol.* **182,** 162–171
34. Tsukui, T., Capdevila, J., Tamura, K., Ruiz-Lozano, P., Rodriguez-Esteban, C., Yonei-Tamura, S., Magallón, J., Chandraratna, R. A., Chien, K., Blumberg, B., Evans, R. M., and Belmonte, J. C. (1999) *Proc. Natl. Acad. Sci. U.S.A.* **96,** 11376–11381
35. Wasiak, S., and Lohnes, D. (1999) *Dev. Biol.* **215,** 332–342
36. Huang, C. J., Tu, C. T., Hsiao, C. D., Hsieh, F. J., and Tsai, H. J. (2003) *Dev. Dyn.* **228,** 30–40
37. Hashimoto, H., Rebagliati, M., Ahmad, N., Muraoka, O., Kurokawa, T., Hibi, M., and Suzuki, T. (2004) *Development* **131,** 1741–1753
38. Diez del Corral, R., Olivera-Martinez, I., Goriely, A., Gale, E., Maden, M., and Storey, K. (2003) *Neuron* **40,** 65–79
39. Diez del Corral, R., and Storey, K. G. (2004) *Bioessays* **26,** 857–869
40. Tickle, C. (2006) *Nat. Rev. Mol. Cell Biol.* **7,** 45–53
41. Niederreither, K., and Dollé, P. (2008) *Nat. Rev. Genet.* **9,** 541–553
42. Osborne, N., and Stainier, D. Y. (2003) *Annu. Rev. Physiol.* **65,** 23–43
43. Peterkin, T., Gibson, A., and Patient, R. (2007) *Dev. Biol.* **311,** 623–635
44. Niederreither, K., Vermot, J., Messaddeq, N., Schuhbaur, B., Chambon, P., and Dollé, P. (2001) *Development* **128,** 1019–1031
45. Kawakami, Y., Raya, A., Raya, R. M., Rodríguez-Esteban, C., and Belmonte, J. C. (2005) *Nature* **435,** 165–171
46. Alexa, K., Choe, S. K., Hirsch, N., Etheridge, L., Laver, E., and Sagerström, C. G. (2009) *PLoS One* **4,** e8261
47. Liang, D., Zhang, M., Bao, J., Zhang, L., Xu, X., Gao, X., and Zhao, Q. (2008) *Gene Expr. Patterns* **8,** 248–253
48. Keegan, B. R., Feldman, J. L., Begemann, G., Ingham, P. W., and Yelon, D. (2005) *Science* **307,** 247–249
49. Waxman, J. S., Keegan, B. R., Roberts, R. W., Poss, K. D., and Yelon, D. (2008) *Dev. Cell* **15,** 923–934
50. Baker, K., Holtzman, N. G., and Burdine, R. D. (2008) *Proc. Natl. Acad. Sci. U.S.A.* **105,** 13924–13929
51. Lopes, S. S., Lourenço, R., Pacheco, L., Moreno, N., Kreiling, J., and Saúde, L. (2010) *Development* **137,** 3625–3632